

# Tissue growth pressure drives early blood flow in the chicken yolk sac

Raphaël Clément<sup>1,\*</sup>, Benjamin Mauroy<sup>1</sup>,  
Annemiek J.M. Cornelissen<sup>2,+</sup>

<sup>+</sup>annemiek.cornelissen@univ-paris-diderot.fr

<sup>1</sup>Laboratoire J.-A. Dieudonné  
University Nice Sophia-Antipolis and CNRS UMR 7351  
Parc Valrose  
06608 Nice Cedex 2 - France

<sup>2</sup>Laboratoire Matière et Systèmes Complexes (MSC)  
University Paris Diderot and CNRS UMR 7057  
10, rue Alice Domon et Léonie Duquet  
75205 Paris Cedex 13 -France

\*Raphaël Clément is currently working at  
Institut de Biologie du Développement de Marseille (IBDM)  
CNRS UMR 7288  
Case 907 – Parc Scientifique de Luminy  
13288 Marseille Cedex 9 – France

Running title: Tissue growth pressure drives early blood flow

Keywords: vascular morphogenesis, hemodynamics, vasculogenesis, tissue mechanics, chicken embryo, sinus vein

## Abstract

**Background** - Understanding how molecular and physical cues orchestrate vascular morphogenesis is a challenge for developmental biology. Only little attention has been paid to the impact of mechanical stress caused by tissue growth on early blood distribution. Here we study the peripheral accumulation of blood in the chicken embryonic yolk sac, which precedes sinus vein formation.

**Results** - We report that blood accumulation starts prior to heart-induced blood circulation. We hypothesized that the driving force for the primitive blood flow is a growth-induced gradient of tissue pressure in the yolk sac mesoderm. Therefore, we studied embryos in which heart development was arrested after two days of incubation, and found that yolk sac growth and blood peripheral accumulation still occurred. This suggests that tissue growth is sufficient to

initiate the flow and the formation of the sinus vein, whereas heart contractions are not required. We designed a simple mathematical model which makes explicit the growth-induced pressure gradient and the subsequent blood accumulation, and show that growth can indeed account for the observed blood accumulation.

**Conclusions** - This study shows that tissue growth pressure can drive early blood flow, and suggests that the mechanical environment, beyond hemodynamics, can contribute to vascular morphogenesis.

## Introduction

Understanding how vascular networks are established during embryogenesis is a great challenge of developmental biology and a major field of investigation. During a process called vasculogenesis (Eichmann et al. 2005, Swift & Weinstein 2009) mesodermal cells differentiate into blood and endothelial progenitor cells or ‘angioblasts’. They cluster and form blood islands that undergo further morphogenesis to form endothelial tubular networks, the so-called capillary plexus. Sprouting angiogenesis and intussusceptive angiogenesis (Djonov et al. 2000, Potente et al. 2011, Ribatti & Crivellato 2012) allow the capillary plexus to expand. This lattice of small vessels prefigures the future hierarchic vascular network. By remodeling of the vessel wall (le Noble et al. 2004, Swift & Weinstein 2009) and by disconnecting side branches from the remodeling vessels (le Noble et al. 2005, Nguyen et al. 2006) this primitive network matures into a hierarchical, functional network with arteries, capillaries and veins. In the last two decades many studies have shown that these processes are established by molecular signaling pathways that involve genetically determined mechanisms (for reviews see Park et al. (2013), Ribatti (2006)) and hemodynamics (le Noble et al. (2004), Lucitti et al. (2007), Nguyen et al. (2006), for a review see Jones et al. (2006)). That the local mechanical environment, and in particular shear stress exerted by the flowing blood, is involved in the remodeling of vascular networks has long been recognized (Thoma 1893). Biophysical models of both plexus formation (Ambrosi et al. 2005) and vascular wall remodeling (Rachev et al. 1996, Taber 1998) have been proposed, but very little attention has been given to the contribution of mechanical stress exerted by the surrounding growing tissue on vascular morphogenesis. A mechanical model for the formation of the capillary plexus was developed by Manoussaki and colleagues (Manoussaki et al. 1996). In their model, they were able to reproduce in vitro cellular patterns emerging from the interaction between traction forces of endothelial cells and the elasticity of the extracellular matrix. In a model study using a diffusion limited aggregation approach, Nguyen et al (Nguyen et al. 2006) suggested that, besides blood flow, stress generated by tissue growth might deform the blood vessels. They further proposed that such a deformation of blood vessels might be essential to remodel the capillary plexus in a realistic arterial pattern. The same group suggested that remodeling in the vicinity of newly formed arteries might mechanically prepattern venous development in the capillary plexus (Al-Kilani et al. 2008). More recently it was observed that stretch in the chicken chorioallantoic membrane induces axial growth and realignment of conducting vessels as well as intussusceptive and sprouting angiogenesis in the capillary bed (Belle et al. 2014).

In this paper, we investigate how yolk sac growth pressure drives blood to the area where the sinus vein will form during early chicken embryogenesis before the heart beats strong enough to pump blood around.

In the following, we refer to the different developmental stages of the chicken as proposed by Hamburger and Hamilton (HH), (Hamburger & Hamilton 1951) or, occasionally, we refer to the days of development (E) after the egg is laid. The yolk sac is an exembryonic tissue surrounding the developing embryo that provides it with nutrients (Fig. 1). The yolk sac is formed (Bauer et al. 2013, Romanoff 1960, Sheng 2010, Eichmann et al. 2005) by rapidly dividing ectodermal cells that start to spread from the embryo over the surface of the yolk. Closely behind the migrating front, between the yolk surface and the ectoderm, the proliferating endodermal epithelial cells of the yolk sac follow the ectodermal cells and form a tight epithelial layer in close contact with the yolk. Mesodermal cells from the splanchnic mesoderm migrate into the space between the ectodermal and endodermal layers from stage HH2 to at least HH9 (Sheng 2010). During and after migration the precursor cells of endothelial and haematopoietic cells cluster into so called blood islands. Earliest blood islands are observed at stage HH6. The cells located at the blood island's edges differentiate into endothelial cells and the cells inside differentiate into haematopoietic cells (Sabin 1920). Soon after differentiation, starting at HH9-10 (Sheng 2010), the endothelial cells anastomose to form the capillary plexus. When the capillary plexus forms, the blood cells are still adhering to each other and to the endothelial cells (Sabin 1920). From stage HH10-11 they start to segregate into individual blood cells (Sheng 2010). At HH12 the heart starts to contract sufficiently to allow individual blood cells to circulate and subsequently the plexus remodels progressively into a hierarchical network by the processes described above. Blood circulating in the yolk sac flows towards the periphery of the area vasculosa (Fig. 1) of the yolk sac, where the sinus vein has formed (Fig. 2A3-5). From there it eventually flows back to the heart first through the cranial vein, later also through the caudal vein. The area vitellina (Fig. 1) is the area of the yolk sac where the mesodermal tissue with blood vessels has not yet entered between the endodermal and ectodermal layers. While at stage HH26/27 (E5) the area vitellina covers most of the yolk surface, the area vasculosa reaches only the equator of the egg yolk. By E15 the area vasculosa fully covers the yolk and the area vitellina has disappeared.

We report here that prior to circulation and subsequent remodeling of the capillary plexus into arteries and veins, around stage HH12, a preliminary accumulation of blood in the distal area vasculosa of the yolk sac precedes the formation of the so-called sinus vein. We propose that this early radial blood flow is caused by a radial tissue pressure gradient associated to growth in the yolk sac tissue. Considering the yolk sac mesoderm growth as a 2D viscous flow, we infer the pressure gradient in the tissue directly from quantitative growth rate measurements performed by Particle Image Velocimetry (PIV). Then, modeling blood flow in the capillary plexus as a porous flow, we show that the tissue pressure gradient can indeed cause a radial flow, eventually leading to peripheral blood accumulation. To confirm that tissue growth alone is sufficient to initiate blood accumulation, we sought experimental conditions in which the role of tissue growth could be isolated. As it has been long known, growth of the yolk sac does not require the embryo to be alive (Romanoff 1960). In eggs in which the heart development was arrested by incision on the second day after incubation at HH11, we found indeed that the yolk sac tissue still grows for about 9 hours. We observed that peripheral blood accumulation still occurs in these eggs. The model simulations signify that the tissue pressure gradient built up by the growth of the tissue is sufficient to allow blood to accumulate at the periphery of the area vasculosa.

Although tissue growth pressure is proposed to play a role in vascular morphogenesis (Nguyen et al. 2006, Al-Kilani et al. 2008) it was to our knowledge not demonstrated that tissue growth pressure can be sufficient to drive blood flow. We propose that this simple physical mechanism induces peripheral blood accumulation that precedes sinus vein formation. More generally, this work illustrates that the impact of the physical environment on the formation of the primitive vasculature might extend to more than hemodynamics, for instance here to tissue pressure gradients caused by tissue growth.

## Results

### Sinus vein formation

The formation of the sinus vein is shown in a timelapse Fig. 2A and the movie M1. Images were taken with a one minute interval for almost 20h, approximately depicting the course of stages HH11 to HH14. The formation of the sinus vein starts with accumulation of blood in the periphery of the area vasculosa of the yolk sac. This blood accumulation starts to become visible around the same time as the contraction of the heart becomes visible, after 4h of growth (Fig 2A2 and the blue line in Fig. 2D and in the movie, M1). Remodeling of the capillary plexus into larger vessels starts approximately after 6.5h of growth (Fig. 2A3-4 and Movie M1). The increasing volume of blood accumulated at the yolk sac periphery (Fig. 2A2-A3, movie, M1) suggests that an outward radial flow of blood exists in the primitive lattice before the heart contracts with enough strength to make the blood circulate. The accumulation of blood leads eventually to the formation of the sinus vein. Upon circulation, the primitive lattice is remodeled as flow increases in the vitelline arteries, and the venous return is established through the cranial vein (A4-A5). By then blood clusters have completely disappeared and individual blood cells circulate in the vasculature.

### Tissue growth causes a radial stress gradient

We hypothesize that the accumulation of blood at the yolk sac periphery is driven by a gradient of mechanical stress caused by tissue growth. In this section we will develop the equations relating growth to tissue pressure and provide measurements of growth.

The yolk sac mesoderm at stages HH11- HH15 is an about  $35\mu\text{m}$  thick layer (Mobbs & McMillan 1979). Mesenchymal tissues are viscoelastic materials with an elastic response at short time scales (seconds) and a viscous response at long time scale (Forgacs et al. 1998, Gonzalez-Rodriguez et al. 2012). As tissue growth is slow as compared to the elastic response, we will model the growth of the yolk sac mesodermal tissue as a viscous hydrodynamic flow between the endodermal and ectodermal layers. Hydrodynamics has been shown to be a relevant framework to describe tissue morphogenesis at developmental time scales (Popović et al. 2016, He et al. 2014). We thus assume that the mesoderm flows between the ectodermal and endodermal layers, which we assume static since they move slowly compared to the mesoderm. In the absence of growth, the local mass balance implies that the divergence of the velocity field  $\vec{u}_t$  of the tissue is zero: what comes out of an arbitrary volume, is equal to what comes in. In presence of growth, new tissue is created inside the volume and the balance should include a growth rate. In that case, a non-zero divergence equation can accurately account for tissue growth (Clément & Mauroy 2014), and the divergence is instead equal to the growth rate  $g(r,t)$ . Assuming the system is axisymmetric

and neglecting the thickening of the tissue, the so-called continuity equation in the yolk sac mesoderm thus reads:

$$\text{div } \vec{u}_t(r, t) = \frac{1}{r} \frac{\partial}{\partial r} (ru_t(r, t)) = g(r, t). \quad (1)$$

We hypothesize that from stage HH11 yolk sac mesoderm grows by proliferation of cells and production of extracellular matrix, since at this stage mesodermal cells entering the yolk sac by migration are negligible. In the absence of specific spatial cues controlling growth in the yolk sac, the growth rate  $g$  should be, to a first approximation, spatially homogeneous. To test this, we predict the evolution of the distance between any two points of the yolk sac in case of homogeneous growth, and compare it with experimental data. If  $g$  is spatially constant, integrating Eq.1 yields:

$$\vec{u}_t(r, t) = \frac{1}{2} g(t) r \vec{e}_r, \quad (2)$$

and the distance  $l$  between any two points in the tissue should increase as:

$$\frac{dl}{dt} = \frac{1}{2} g(t) l. \quad (3)$$

To measure the velocity of the yolk sac mesoderm we used digital Particle Image Velocimetry techniques (dPIV, Cardoso 2013). Up to stage HH12 we tracked blood aggregates. The aggregates reside either in the blood islands or in the developing capillary plexus. When the circulation starts and blood vessels can be distinguished we used vascular bifurcations as markers for mesodermal tissue growth. The markers are indicated in the movie (M1) with orange circles. The individual tracks of the markers up to 7.5h are shown in Fig. 2B. For each pair of markers, we measured the distance  $l$  as a function of time, as well as the distance increase rate  $\Delta l / \Delta t \approx dl/dt$  (see experimental procedures section). The results do follow a linear trend (Fig. 2C), and the slope of the linear fit provides a measurement of  $g$  at time  $t$  (Eq.3). Repeating this procedure over the entire experiment, we were able to measure how  $g$  varies over time (Fig. 2D). Fig 2D shows that the growth curve measured by tracking the blood aggregates (black line) is consistent with the growth curve measured by tracking vascular bifurcations (green line). This suggests that the blood aggregates indeed don't move relatively to the endothelial cells of the capillary plexus, as described by Sabin (Sabin 1920) who observed that the blood aggregates in the plexus adhere to the endothelial cells. Therefore, the movements of both markers seem to reflect well the growth of the mesoderm. The coefficient of determination for the linear fit (Fig. 2C) is low because of the noise in determining the displacement of the markers using the dPIV algorithm, resulting in a large spread of distance increase rates as a function of distance between the markers. Therefore, as an additional control, we used the measurement of the growth rate  $g(t)$  to predict how the yolk sac should expand. To do so we applied Eq.3 to a series of points at the moving front of the mesoderm, paired with their center of mass which is not moving with time. We then superimposed their predicted trajectories (Movie M1, yellow squares) to the movie. The good agreement between predicted and actual expansion confirms that the time dependent, but spatially homogeneous growth rate  $g(t)$  is a good approximation.

Since the mesoderm consists in a thin layer growing between the static ectodermal and endodermal layer, we can use the hydrodynamic analogy of plane flow between two parallel

plates to approximate the pressure field in the mesoderm. The local gradient of tissue pressure  $p$  exerted by growth reads:

$$\overrightarrow{\text{grad}} p_t(r, t) = -\frac{8\eta_t}{Ah^2} \overrightarrow{u}_t = -\frac{4\eta_t g(t)}{Ah^2} r \overrightarrow{e}_r, \quad (4)$$

with  $A$  and  $h$  depending on the velocity profile in the mesoderm.  $A$  is the ratio between the mean velocity,  $u_t$ , and the maximum velocity.  $A = 2/3$  for a parabolic flow profile (Poiseuille flow) and  $A = 1$  for a perfect plug flow.  $h$  is the total height on which there is a shear. With  $H$  being the thickness of the yolk sac mesoderm, then  $h = H$  for a parabolic flow and  $h = 0$  for a perfect plug flow ( $A = \frac{3H-h}{3H}$ , see supplemental materials for details).  $\eta_t$  is the tissue viscosity in the sheared layers  $h$  at long time scales. For a parabolic flow  $\eta_t$  represents the global tissue viscosity. The actual shape of the tissue velocity profile is unknown and depends on the friction the yolk sac tissues encounter. There are two sources of friction: the friction inside the tissue between the mesodermal cells and the friction between the mesoderm and the ecto- and endodermal layers. When they are approximately the same, or when the friction between the mesodermal cells is lower, it approaches a parabolic velocity profile. When there is more friction between the mesodermal cells than at the interfaces, the velocity profile flattens up. At the extreme it can reach a perfect plug flow. The pressure gradient derived from a hydrodynamics parabolic flow is then the lower possible limit, and when the tissue becomes more rigid the pressure gradient can become much larger.

Assuming that the pressure at the yolk sac circumference ( $r = R_{AV}$ ) is constant and equal to  $p_0$ , the pressure field thus reads:

$$p_t(r, t) = p_0 + \frac{2\eta_t g(t)}{Ah^2} (R_{AV}(t)^2 - r^2), \quad (5)$$

where  $R_{AV}(t)$  is the radius of the area vasculosa of the yolk sac at time  $t$ . Hence the pressure caused by tissue growth in the yolk sac mesoderm is higher in the proximal yolk sac than near the outer border, and increases as the yolk sac grows. This is rather intuitive since confinement is higher close to the center. The velocity and pressure fields caused by tissue growth alone are schematized Fig. 3.

### **Tissue growth is sufficient for blood accumulation**

Let us now investigate how tissue growth pressure impacts the blood flow. As we showed above, the aggregates do not move relatively to the plexus and we assume that only free flowing blood passes through the capillary plexus in between the aggregates. Blood is generated by the production of plasma by the endothelial cells followed by segregation of individual blood cells from the aggregates (Ferkowicz & Yoder 2005, Sabin 1920). To model their flow generated by the growth-driven tissue pressure, we assume that blood flows in the capillary plexus in between the aggregates as in a porous medium. This is justified since yolk sac geometry changes due to growth are slow compared to the motion of blood. This also assumes that space for blood transport in the capillary plexus is not deformed by the blood flow. The effective permeability, considering that the transport space is randomly oriented is given by  $\kappa = \psi b / 96$  (Guyon et al. 2001).  $\psi$  is the volume fraction of the space available for blood transport in the mesodermal tissue, and  $b$  the typical pore size. Flow in a medium with heterogeneous pore size is limited by the smallest pores, hence we assume  $b$  to be the typical

diameter of capillaries. Darcy's law relates the velocity  $\vec{u}_b$  of the porous flow of blood with the gradient of growth pressure:

$$\vec{u}_b = -\frac{\kappa}{\eta_b} \overrightarrow{\text{grad}p}_t, \quad (6)$$

with  $\eta_b$  being the viscosity of blood. Using Eq.4 and substituting  $\kappa$  in Eq.6 yields:

$$\vec{u}_b = \frac{\psi b^2 \eta_t}{24 A h^2 \eta_b} g(t) r \vec{e}_r = \frac{1}{2} \psi C g(t) r \vec{e}_r, \quad (7)$$

with  $C$  being the dimensionless tissue-blood resistance ratio. Note that  $\vec{u}_b$  is the velocity of the blood relative to the tissue. In an external frame of reference, the tissue is also in motion, with velocity  $\vec{u}_t$ , and total blood velocity equals  $\vec{u}_b + \vec{u}_t$ . This suggests that because of growth pressure, blood in the capillaries will flow faster than the tissue itself, and therefore might accumulate at the periphery. To test that blood can indeed accumulate at the periphery because of tissue growth alone, we designed experimental conditions in which the effect of growth could be isolated, in particular from the pressure generated by heart contractions. It has been long known that eggs in which the embryo dies can still display yolk sac growth (see (Romanoff 1960) and references therein). Therefore we studied embryos ( $n = 3$ ) in which heart development was arrested by incision on the second day after incubation at HH11, before heart contraction was large enough to allow blood to remodel the capillary plexus. As expected, in all cases, the yolk sac not only survives but also continues to grow for some time (Fig. 4A and Movie 2). In the absence of heart-driven blood flow through the vitelline arteries, no remodeling of the primitive blood lattice is observed, and the majority of blood cells remain organized in aggregates. This confirms that shear stress caused by the blood circulation is crucial for vascular remodeling, as abundantly reported in literature (Lucitti et al. 2007, Garcia & Larina 2014). In addition, we observe that yolk sac peripheral blood accumulation also occurs, which shows that heart contractions or subsequent blood flows are not required for peripheral blood accumulation.

We also quantified the growth rate using dPIV (Fig. 4B, 4C and Movie 2). Note that the same controls, involving predictions of yolk sac expansion, were performed (Movie 2). To compare the yolk sac growth of the control embryo with the incised embryo, we shifted the growth curve of the control to have the same initial growth rate for both cases. Note that at this time, the yolk sac area is also similar in both the control and the incised embryos. Our quantifications show that yolk sac growth was slower than in the control embryo:  $g(t)$  slows down slower, but drops to zero and eventually becomes negative as growth stops and the yolk sac shrinks, while the control yolk sac continues to grow at a rate of  $0.05h^{-1}$  (Fig. 4D).

In addition, we measured the average width of the stripe of accumulated blood at the periphery in both control and incised eggs after 7.5 hours. We found that it was about 0.18mm in the former while it was slightly smaller, about 0.16mm, in the latter (Figure 5A). Width of the blood accumulation was measured as described in the experimental procedures section.

## Simulations

To test whether our theoretical model could qualitatively account for our experimental observations, we designed simulations of blood transport in the yolk sac tissue. For the sake of simplicity, we used an axisymmetric description and modeled the presence of free flowing

blood in the yolk sac using the blood volume fraction in the tissue as a single local parameter  $\alpha(r,t)$ . In between the blood aggregates in the capillary plexus blood cells and plasma can flow, which we refer to as free flowing blood.  $\alpha(r,t)$  is defined as the average ratio between the volume of this free flowing blood and the total mesodermal tissue volume at distance  $r$  from the center of the embryo. In other words, if one draws a ring of infinitesimal width  $dr$  at radius  $r$  in the yolk sac, a fraction  $\alpha(r,t)$  of its volume is occupied by blood. Since we defined  $\psi$  as the volume fraction available for blood transport between the blood aggregates in the capillary plexus, we will assume in the following that this space is filled with blood cells and plasma, and thus that  $\psi = \alpha$ .

We seek to describe the time evolution of the fraction of blood in the tissue  $\alpha(r,t)$  in the growing area vasculosa of the yolk sac. Locally,  $\alpha$  variation results from the transport of blood at velocity  $\vec{u}_b + \vec{u}_t$ , and from the creation rate of free flowing blood  $g_\alpha$ . The source for blood cells in the free flowing blood are the blood aggregates. Blood plasma is produced by the endothelial cells of the anastomosed blood islands (Ferkowicz & Yoder 2005, Sabin 1920). The continuity equation for  $\alpha(r,t)$  thus reads:

$$\frac{\partial \alpha}{\partial t} = \underbrace{g_\alpha}_{\text{new blood}} - \underbrace{\text{div}(\alpha(\vec{u}_b + \vec{u}_t))}_{\text{blood transport}}. \quad (8)$$

For the sake of simplicity, we chose the blood production,  $g_\alpha$  to be independent of position ( $r$ ) and time ( $t$ ):  $g_\alpha = cst > 0$ , and the initial amount of free flowing blood to be zero:  $\alpha(r, 0) = 0$ . This is obviously an oversimplification, which we will address in the discussion section. Blood transport is limited by the outer border of the area vasculosa of the yolk sac, located at radius  $R_{AV}(t)$ . Near the periphery, blood velocity  $u_b(R_{AV}(t))$  is higher than tissue velocity, hence blood is accumulating. During a short time  $dt$ , blood near the periphery travels a small distance  $dr = u_b(R_{AV}(t))dt$ . Therefore, during time  $dt$ , the blood located between the radii  $R_{AV}(t) - dr$  and  $R_{AV}(t)$  reaches the periphery and contributes to the accumulation. Then, accounting for a circular yolk sac with thickness  $H$ , and for an inner blood fraction in the tissue of  $\alpha(R_{AV}(t), t)$ , the volume  $dV$  of blood accumulating at the periphery during  $dt$  is:

$$dV = 2\pi R_{AV}(t) \times H \times u_b(R_{AV}(t)) dt \times \alpha(R_{AV}(t), t). \quad (9)$$

The total volume of blood accumulated at the periphery at time  $t$  is then simply  $V(t) = \int_0^t dV$ .

In the simulations, the displacement of the tissue boundaries, the boundary between the area pellucida ( $R_{ZP}(t)$ ) and the area vasculosa and the boundary between the area vasculosa and the area vitellina ( $R_{AV}(t)$ ) is set by the growth rate  $g(t)$  measured earlier, using Eq. 2. The spatio-temporal evolution of  $\alpha(r,t)$  is calculated within these moving boundaries using Eq. 8 and Eq. 7. From there the volume increase  $dV$  of blood accumulating at the periphery is obtained at each time step. Importantly, the value of the growth rate  $g(t)$  is plugged directly from our experimental measurements.

The parameters used for the numerical resolution of the sinus vein width comprise the tissue-blood resistance ratio,  $C$ , the free blood creation rate,  $g_\alpha$ , the tissue growth rate,  $g(t)$  and the initial conditions for the radius at the yolk sac zona pelucida,  $R_{ZP}(0)$ , the radius of the yolk sac at the area vasculosa,  $R_{AV}(0)$  and the free blood volume fraction,  $\alpha(r, 0)$ . The value

for parameter  $C = \frac{b^2 \eta_t}{12Ah^2 \eta_b}$  is estimated from the literature. There is no quantitative data available for the tissue velocity profile (the parameters  $h$  and  $A$ ) nor for the viscosity in the shear layers of the mesodermal tissue ( $\eta_t$ ). But blood pressure measured in the vitelline artery just when the primitive heart starts to contract at HH12 (Hu & Clark 1989) provides us the order of magnitude of tissue pressure close to the embryo. Therefore, in Equation 5 we introduce the resistance to tissue flow:  $\Omega_t = \frac{8\eta_t}{Ah^2}$ . Using the measured growth rate  $g(t)$  in the control situation, the tissue resistance is tuned such that the temporal average of tissue pressure at  $r = R_{ZP}$  is equal to 0.03 kPa, the diastolic pressure in the vitelline artery at HH12 (Hu & Clark 1989). The parameters related to the resistance to blood flow, blood viscosity ( $\eta_b$ ) and the effective pore size ( $b$ ), are also unknown at these early embryonic stages, but their values are extrapolated from the available literature at later embryonic stages as argued in the supplemental materials.

The tissue growth rate,  $g(t)$ , the radii  $R_{AV}(0)$  and  $R_{ZP}(0)$  are measured (Fig. 2C and 4C).

The parameters related to blood production, the initial free blood volume fraction,  $\alpha(r, 0)$ , is assumed to be zero and the blood production rate,  $g_\alpha$  is tuned such that it simulates the measured width of the sinus vein as explained in the following.

Numerical simulations confirm that blood is indeed transported towards the periphery and that the total volume  $V(t)$  accumulated at the periphery increases over time. We can estimate the typical width  $w(t)$  of the peripheral ring of blood:

$$w(t) = \frac{V(t)}{2\pi H R_{AV}(t)}. \quad (10)$$

In the incised embryo, we measured that at 7.5 hours, the typical width of the peripheral blood accumulation was 0.16 mm (Fig. 5A2). In the model we calibrate  $g_\alpha$  such that  $w = 0.16$  mm after 7.5 hours growth of the incised embryo. Using the same parameters except for the experimentally measured growth rate, the model predicts that  $w = 0.24$  mm in the control embryo as compared to a measured width of 0.18 mm (Fig. 5A1). The calibration of  $g_\alpha$  yields a value of  $0.027 h^{-1}$ .

A table including all physical parameters and variables is provided in the experimental procedures section, together with details on the simulation model.

Fig. 5B-E show the distribution of the blood and tissue velocity, the pressure gradient and the tissue fraction of blood for the simulations after 0.5h and 7.5h of growth for the control and incised embryo. The pressure that is built up (Fig. 5D) depends on the tissue growth rate and is around 0.04 kPa at the start of the experiment and reduces to about 0.03 kPa at 7.5h for the control embryo and to 0 for the incised one.

The small pressure gradient is enough to generate a radial blood velocity in the order of mm/h (Fig. 5B). There is only a small fraction of free flowing blood that flows at a very low speed, which explains why it is hard to observe the moving red blood cells experimentally.

To assess whether our estimate of blood production rate,  $g_\alpha$ , is within a reasonable order of magnitude, we can estimate the fraction of red blood cells that accumulate in the sinus vein with respect to the estimated volume of the red blood cells in the blood aggregates, the source

for the blood cells. Roughly, the blood aggregates at  $t = 0$  of the incised embryo occupies 1/5 of the total surface (Fig. 4A2). The estimated volume of blood cells in the aggregates equals thus:  $1/5 \times \pi \times ((R_{AV}(0)^2) - (R_{ZP}(0)^2)) \times H = 0.25mm$ . The simulated blood volume that accumulates in the sinus vein after 7.5h equals 0.28mm. Assuming a hematocrit between 5 and 15%, the accumulated volume of red blood cells in the sinus vein is in between 0.013 and 0.041mm, which represents only 5 to 16% of the blood aggregates. This is consistent with the fact that the blood aggregates do not change much their shape, nor their grey level (which relates to the amount of blood cells in the tissue) in the course of growth of the incised embryos (Fig. 4A and Movie 2).

In addition, the blood production rate  $g_\alpha = 0.027 h^{-1}$  is in the same range as our measurements for the tissue growth rate,  $g(t)$  (Fig. 4D).

Overall, the simulations show that growth-induced tissue pressure can indeed drive an accumulation of blood in the periphery of the yolk sac area vasculosa commensurate with that observed *in vivo*.

## Discussion

The results presented in this paper show that heart-induced flow in the yolk sac is not required to accumulate blood in periphery of the yolk sac area vasculosa, which begins prior to circulation. We proposed that a mechanical pressure gradient caused by homogeneous tissue growth might drive the radial flow of blood that eventually leads to peripheral blood accumulation. This hypothesis is supported by experiments in which the heart is arrested by incision before circulation starts: the yolk sac still grows and the accumulation of blood is still observed. Based on quantitative growth measurements, a simple theoretical model was built that predicts the peripheral accumulation of blood due to tissue growth pressure.

The theoretical model reveals the basic, qualitative mechanisms of peripheral blood accumulation. In the following, we discuss our theoretical assumptions and results and point out limitations.

### Spatially homogeneous growth

Our analyses show that the growth of the yolk sac mesoderm is well described by a spatially homogeneous growth (Fig. 2C and 4C and Movies 1 and 2). This implies that the cells are proliferating at the same rate, independent of their location. Phosphohistone H3 staining, marking all mitotic cells, indicates that at E3 and at E5 yolk sac mitotic cells are distributed homogeneously in the yolk sac (Fig. 6A and B in (Nagai & Sheng 2008)). This shows that the yolk sac is growing spatially homogeneous at these stages. Our analyses suggest that it is also the case at earlier stages (E2, HH11 up to HH14). This likely implies that intussusceptive growth (Djonov et al. 2000) in which the capillary plexus expands by insertion of numerous transcapillary mesodermal tissue pillars is playing an important role, besides sprouting angiogenesis.

### Mesoderm grows between static ecto and endodermal layers

Tissue pressure builds up in the mesoderm, because we assume it is growing between static endo- and ectodermal layers. At stage HH26/27 (E5) (Sheng 2010) the area vitellina, which contains only the ecto- and endoderm covers most of the yolk. At the same time, the area

vasculosa, the part of the yolk sac in which the mesoderm has entered, reaches the equator of the yolk. This implies that from this stage on, the mesoderm is indeed growing in between the static endo- and ectoderm. We think it is reasonable to assume that the mesoderm also grows at earlier stages between the static endo- and ectodermal layers. However, the ectoderm and endoderm are possibly still growing in the area vasculosa. In that case, tissue pressure should still build up due to friction of the endoderm with the yolk, and of the ectoderm with the vitelline membrane.

### **Blood transport takes place in the capillary plexus that reaches out to the periphery of the area vasculosa**

Independent marking at stage HH10 of globin in the blood cells, the blood precursor cells and endothelial cells together with the blood cells (Fig. 2 in (Sheng 2010)), reveals that blood cells are present close to the embryo, but not yet in the periphery, which we also observe in our experiments. However, endothelial cells are already present up to the periphery of the area vasculosa. Thus, at the start of our experiment (at HH11) blood can be transported to the periphery via the capillary plexus.

### **Production of free flowing blood, $g_\alpha$**

Free blood is produced by 'liquefaction' of the blood aggregates: red blood cell dissociation from the aggregates that are carried away by newly produced plasma (Sabin 1920). Blood aggregates are distributed in a U shaped region in the area vasculosa of the yolk sac. Progressive smaller blood islands are observed close to the embryo and expression of hemoglobin occurs initially in the more distal blood islands (Sabin 1920, Sheng 2010). This is proposed to reflect the progressive phase of differentiation (Sabin 1920, Sheng 2010, Eichmann et al. 2005). We also observe such a gradient in our experiments (Fig 2A2 and Fig. 4A2). Therefore, a more realistic description might include a spatio-temporal dependence of free flowing blood production,  $g_\alpha$ . Besides,  $g_\alpha$  might also depend on shear forces which could contribute to the dissociation of red blood cells from the aggregates. Finally,  $g_\alpha$  might be different in control and incised embryos. However, in the absence of quantitative data, we settled for straightforwardness with a homogeneous and constant production of free flowing blood.

### **Width of the sinus vein as a measure for volume accumulation due to tissue growth**

We calibrate the production of free flowing blood ( $g_\alpha$ ) with the width of the sinus vein of the incised embryo after 7.5h hours of growth (see Fig. 5A2). We are aware that the observed width is not perfectly reflecting the amount of blood accumulated in the periphery of the area vasculosa. Besides the subjective measurement of the width, the grey level along the sinus vein is not constant, indicating that not the same amount of blood is accumulated at all positions in the sinus vein. However, sensitivity analyses of the model (Fig. 6A) show that even when we are 50% mistaken with our estimation of the observed sinus vein width, calibration of  $g_\alpha$  would yield a 50% increase / decrease as well, thus remaining within the same order of magnitude.

Using the same values for all parameters except for the experimentally measured tissue growth rate, our model predicts a width of 0.24mm for the control after 7.5h of growth. In the control experiment we measure a width of 0.18mm (Fig. 5A). It should be noted however, that the simulated width is the width predicted without taking into account the pressure build

up by heart contractions and the circulating blood. At  $t = 7.5h$  blood started already to circulate (Fig. 2A4). Therefore, the previously accumulated blood is flowing elsewhere in the circulation, and shear forces remodeling the sinus vein contribute to the establishment of the sinus vein width. The simulated width of the sinus vein reflects thus the volume accumulation as if there was only tissue growth pressure.

### Initial conditions

At the start of our simulations we set the fraction of free flowing blood to zero ( $\alpha(r,0) = 0$ ). This implies that the endothelial cells of the capillary plexus tightly enclose the blood aggregates. That is to say the endothelial cells of the blood islands have just anastomosed. Blood islands anastomose at stage HH9-10 (Sheng 2010). At the onset of our experiments (HH11), we expect that mesodermal tissue growth and production of free flowing blood has already contributed to the accumulation of blood in the periphery of the area vasculosa. In the absence of precise data concerning the presence of free flowing blood ( $\alpha(r,0)$ ) at the onset of our experiments, we carried out a sensitivity analysis for both control and incised embryos (Fig. 6B). It suggests that increasing  $\alpha(r,0)$  requires adjusting our calibration of  $g_a$ , yet within a relatively small range (Fig. 6A). Similarly, for the initial value for the accumulated peripheral volume, expressed in sinus vein width. Initial values in the order of tenth of micrometers would require only a small adjustment of  $g_a$ .

### Resistance to tissue flow vs blood flow

The parameters related to resistance to tissue flow ( $\Omega_t$ ) comprise the velocity profile ratio,  $A$ , the total height of the mesoderm that encounters shear,  $h$ , the mesoderm viscosity in the shear layers at the ecto- and endoderm,  $\eta_t$ . To our knowledge no measurements are available in the current literature that allows us to estimate the values for these parameters. Therefore, we tuned the tissue resistance such that the temporal average of tissue pressure at  $r = R_{ZP}$  is equal to the diastolic pressure in the vitelline artery when the heart starts to contract at HH12 (Hu & Clark 1989). At this stage the heart is still a tube composed of a three- to five-cell myocardial mantle surrounding a cuff of cardiac jelly and a one-cell layer of endocardium (Hu & Clark 1989). At HH12 Hu and Clark measured in the vitelline artery a diastolic pressure of 0.03 kPa and a systolic pressure of 0.04 kPa. The diastolic and systolic pressure increase up to 0.05 kPa and 0.07 kPa resp. at stage HH14. Since the vitelline arterial pressure is the sum of the tissue pressure and the pressure build up by the heart, we assumed that the tissue pressure during our experiment (HH11 - HH14) should not be larger than the vitelline artery diastolic pressure at HH12. If we would assume a parabolic velocity profile, with  $A = 2/3$  and  $h = H$ , the estimated global tissue viscosity would be  $43 Pa \cdot s$ . The viscosity of the mesoderm would then be more than 2 orders of magnitude lower than the viscosity ( $10^4 Pa \cdot s$ ) estimated for cell aggregates of the heart, liver and neural retina of 3.5 - 6 days chicken embryos (Forgacs et al. 1998). However, at low pressure gradients the mesoderm is likely not sheared over the full height and the velocity profile is more flat. I.e. the mesoderm is more rigid because the friction within the mesodermal layer is larger than at the ecto and endodermal interfaces. In case of a perfect plug flow, with  $A = 1$  and  $h \rightarrow 0$ , the pressure gradient diverges for a given velocity and viscosity. Thus we can assume that the friction between the mesodermal layer and the ecto- and endodermal membranes is very small, with a viscosity in the thin shear layers small enough to reach a tissue pressure near the embryo of 0.03 kPa. Possibly, the thin shear layers solely consist of low viscous extracellular matrix. Alternatively, we could have modeled the mesoderm as a solid growing disc with a small

friction between the ecto- and endodermal layers. This would result in a tissue stress gradient, which is analogous to the tissue pressure gradient applied in our viscous approach.

The parameters related to the resistance to blood flow are the blood viscosity  $\eta_b$  and the effective value for the pore size  $b$ . As described in the supplemental materials the values for blood viscosity are quite insecure because direct measurements lack at these early developmental stages.

In the model, blood transport depends on the ratio  $C$  between the two resistances. Yet, Fig. 6C shows that the width of the sinus vein is not dramatically affected when this ratio is modified, even by a factor 10 and even when the mesoderm approaches a plug flow ( $h \rightarrow 0$ ) and  $C$  becomes very large.

The porous model assumes a constant effective value for the pore size  $b$ , being the smallest length scale in which the blood flows, which we assume to be the capillary diameter. The pore size  $b$  could depend on the transmural pressure set by the tissue pressure,  $p_t$ : yet it is likely that a more stressed region will have less space for flow. This feedback might have interesting consequences for the remodeling process. Indeed, a gradient of  $b$  would imply a gradient of hydrodynamic resistance in the yolk sac, thus a higher resistance in the proximal region and a lower resistance in the distal region. This would be in agreement with previous observations of higher vascular densities in the distal yolk sac (Al-Kilani et al. 2008). It might also explain why blood flow does not shunt the distal yolk sac, going directly from the cardiac vitelline outputs to the cardiac cranial and caudal inputs through the proximal yolk sac (Al-Kilani et al. 2008).

### **Thickening of the mesodermal tissue**

In the model we neglect the thickening of the mesodermal tissue. Measurements on the evolution of the thickness lack. If the tissue becomes thicker, it would imply more growth than that we account for in our 2D approach. Due to transverse resistance, this extra growth would result locally in a larger tissue pressure. Assuming that the tissue close to the embryo would grow thicker than at the periphery would create a larger pressure gradient than expected solely from the 2D approach. In the same time, with a transverse parabolic flow profile, increasing tissue thickness would decrease the resistance to tissue flow, decreasing the pressure gradient. However, we expect that this latter effect is negligible when the tissue flow approaches a plug profile.

### **Conclusion**

While these remarks show the quantitative limits of the theoretical model, we believe that it provides, together with the experiments, a proof of principle that blood accumulation at the periphery prior to perfusion is driven by a gradient of mechanical stress caused by tissue growth. Altogether, the results presented here tend to draw a global picture of vascular morphogenesis in the chicken yolk sac: prior to perfusion, tissue pressure caused by growth initiates a radial blood movement, and blood accumulates at the yolk sac periphery. Upon perfusion, increased shear leads to the remodelling of the capillary plexus into a hierarchised network. Obviously, the peripheral accumulation of blood stops as soon as the venous return is established, since blood can flow back to the heart. The radial pressure gradient might also cause a permeability gradient, which might prevent the blood flow to shunt the distal regions of yolk sac.

It also provides a general temporal picture: The capillary plexus forms and free flowing blood starts to be produced while the tissue is still growing. The pressure gradient due to growth pushes the blood outward, and starts the accumulation in periphery of the area vasculosa of the yolk sac. These movements can be taken over by the increasing efficiency of the heart, to allow blood to circulate, while finally the yolk sac growth stops and the associated pressure gradient vanishes. The timing of both events has to be well tuned as in a successful relay race. Such a precise timing of development of peripheral vascular networks and its connection to the heart might be a general developmental strategy.

In conclusion, this work constitutes a first step towards the understanding of how tissue growth pressure can drive blood flow in the yolk sac mesoderm. It introduces basic ideas, directions and tools for future investigations. It also illustrates that the mechanical environment beyond mere hemodynamics might play a role in patterning the primitive vascular system, and in particular that tissue growth can cause pressure gradients large enough to drive blood flows. While the model system chosen here has a very basic geometry and therefore simple flow patterns, such a mechanical feedback between growth and vascular morphogenesis is likely to underlie, in more subtle geometries, the formation of complex vascular patterns.

## **Experimental Procedures**

### **Experimental Preparation**

Fertile chick eggs (Lohmann Brown eggs) were obtained from CAIF (47 rue d'Aulnay - Moulin Fourcon - 91180 Saint Germain Les Arpajon - France) and stored at 15 degrees C. After 50h of incubation at 37 degrees C a window in the egg shell was cut and the egg was placed in a mini-incubator (minitube HT300 controller with 2 heating plates) for timelapse observation (macrofluvo Leica Z16 equipped with a Fastcam SA3, Photron camera). Images were taken using epi-illumination with a blue filter (Schott KL 1500 LED) with a one minute interval. For the incised embryos, heart development was arrested by incision of the embryo before placing the egg in the mini-incubator. Before incision we verified if the embryo was normally developed up to stage HH10-11. At this stage the heart is still a single tube and not yet fully developed. In our experimental settings we cannot distinguish the primary heart, but with fine surgical scissors we cut the embryo in a transverse plane in two pieces at the level of where the heart would develop, leaving the yolk sac around intact. Control embryos were left intact.

### **Data analysis**

To measure the velocity field of the yolk sac mesoderm we used the moving blood islands and vascular bifurcations as markers. In the first image (at  $t = 0$ ), for both the control and the incised embryo, the blood islands in the yolk sac are marked manually using the point selection tool of imageJ (Rasband 1997). Digital particle image velocimetry (dPIV, imageJ plugin (Cardoso 2013) was used to obtain the position of our markers in each subsequent image (the time interval between images equals 1'). Blood islands were tracked till  $t = 15h59'$  for the incised embryo and till  $t = 8h34'$  for the control embryo. In the yolk sac of the control embryo there is a transition from blood islands to the vascular network. Therefore we marked manually the bifurcations at  $t = 6h41'$  and used the dPIV imageJ plugin to determine the position of the bifurcations in each subsequent image up to  $t = 18h56'$ .

To estimate the growth rate  $g(t)$ , we first computed the distance  $l$  at time  $t$  between each pair of markers. Then we calculated the distance increase rate  $dl/dt$  at time  $t$  on a  $\Delta t = 30'$  window:  $dl/dt \simeq \Delta l/\Delta t = [l(t + 15) - l(t - 15)]/30$ . Growth  $g$  at time  $t$  was finally estimated from the slope of the linear regression line between  $l(t)$  and  $dl/dt$ , using Equation 3 in the Results section. Besides the slope, the coefficient of determination ( $r^2$ ) of the regression line was calculated. This was repeated for all time points throughout the time lapse observation.

To double check that homogeneous growth is a good approximation, we manually marked a number of points on the moving front of the mesoderm (the border between the area vasculosa and area vitellina). Assuming that the center of mass of these points moves the same as the center of mass of the dPIV trajectories, we could, by using Equation 3 in the Results section and our estimate of the growth rate  $g(t)$ , predict the position of the moving front of the mesoderm at all time points in both control and incised embryos (see supplemental movies M1 and M2).

The width of blood accumulation at the periphery of area vasculosa was measured for both control and incised embryos. This is illustrated for a small section in Figure 5A. The coordinates of the inner and outer boundaries were obtained by eye (yellow dotted lines in Figure 5A) using the polygon tool of imageJ (Rasband 1997). With Matlab, the shortest distance from each point on the outer polygon line to the inner polygon line was obtained (green bars in Figure 5A). Width was then calculated averaging the shortest distances.

## Model

The transport model for  $\alpha$  writes:

$$\frac{\partial \alpha}{\partial t} = g_\alpha - \text{div}(\alpha(\vec{u}_b + \vec{u}_t)). \quad (11)$$

$C = \frac{b^2 \eta_t}{12 A h^2 \eta_b} = \frac{\Omega_t b^2}{96 \eta_b}$ , the ratio of the resistance against tissue flow vs. the resistance against blood flow. We have  $u_t = gr/2$  and  $u_b = C\alpha gr/2$ . Therefore the transport equation writes:

$$\frac{\partial \alpha}{\partial t} = g_\alpha - \frac{1}{2} \text{div}((\alpha + C\alpha^2)gr\vec{e}_r), \quad (12)$$

which leads to:

$$\frac{\partial \alpha}{\partial t} = g_\alpha - (\alpha + C\alpha^2)g - \left(\alpha C + \frac{1}{2}\right)gr \frac{\partial \alpha}{\partial r}, \quad (13)$$

which we solve numerically on growing boundaries,  $R_{ZP}(t)$  and  $R_{AV}(t)$ . Boundaries displacements are simply fixed by the tissue velocity  $u_t$ . All parameters can be found in Table 1.

## Acknowledgements

We thank Stéphane Douady, Sylvie Lorthois and Vincent Fleury for contributing to interesting discussions about the interpretation of the experimental data and the theory. This project was funded by CNRS grant "Projet Exploratoire Premier Soutien - Physique Théorique et ses Interfaces" (PEPS PTI 2012 and 2013); and by City of Nice grant "Aide

Individuelle aux Jeunes Chercheurs” (2012). A travelling grant for R. Clément was funded by ”Interactions Committee” of laboratory J.-A. Dieudonné (2014).

## References

- Al-Kilani, A., Lorthois, S., Nguyen, T.-H., le Noble, F., Cornelissen, A., Unbekandt, M., Boryskina, O., Leroy, L. & Fleury, V. 2008. During vertebrate development, arteries exert a morphological control over the venous pattern through physical factors. *Phys. Rev. E Stat Nonlin Soft Matter Phys.* 77 (5 Pt 1): 051912.
- Ambrosi, D., Bussolino, F. & Preziosi, L. 2005. A review of vasculogenesis models. *Journal of Theoretical Medicine* 6(1): 1–19.
- Bauer, R., Plieschnig, J. A., Finkes, T., Riegler, B., Hermann, M. & Schneider, W. J. 2013. The developing chicken yolk sac acquires nutrient transport competence by an orchestrated differentiation process of its endodermal epithelial cells. *J. Biol. Chem.* 288(2): 1088–1098.
- Belle, J., Ysasi, A., Bennett, R. D., Filipovic, N., Nejad, M. I., Trumper, D. L., Ackermann, M., Wagner, W., Tsuda, A., Konerding, M. A. & Mentzer, S. J. 2014. Stretch-induced intussusceptive and sprouting angiogenesis in the chick chorioallantoic membrane. *Microvascular Research* 95(0): 60 – 67.
- Cardoso, O. (2013), DPIV ImageJ plugin, V 7-2-2013, Laboratoire Matière et Systèmes Complexes (MSC) University Paris Diderot and CNRS UMR 7057, France.
- Clément, R. & Mauroy, B. 2014. An archetypal mechanism for branching organogenesis. *Physical biology* 11(1), 016003.
- Djonov, V., Schmid, M., Tschanz, S. A. & Burri, P. H. 2000. Intussusceptive angiogenesis: its role in embryonic vascular network formation. *Circ. Res.* 86(3): 286–292.
- Eichmann, A., Yuan, L., Moyon, D., le Noble, F., Pardanaud, L. & Breant, C. 2005. Vascular development: from precursor cells to branched arterial and venous networks. *Int J Dev Biol* 49: 259–267.
- Ferkowicz, M. J. & Yoder, M. C. 2005. Blood island formation: Longstanding observations and modern interpretations. *Experimental Hematology* 33(9 SPEC. ISS.): 1041–1047.
- Forgacs, G., Foty, R. A., Shafrir, Y. & Steinberg, M. S. 1998. Viscoelastic properties of living embryonic tissues: a quantitative study. *Biophysical journal* 74(5): 2227–2234.
- Garcia, M. D. & Larina, I. V. 2014. Vascular development and hemodynamic force in the mouse yolk sac. *Frontiers in Physiology* 5: 308.
- Gonzalez-Rodriguez, D., Guevorkian, K., Douezan, S. & Brochard-Wyart, F. 2012. Soft matter models of developing tissues and tumors. *Science* 338(6109): 910–917.
- Guyon, E., Hulin, J.-P., Petit, L. & Mitescu, C. D. 2001. *Physical Hydrodynamics*. Oxford University Press.
- Hamburger, V. & Hamilton, H. 1951. A series of normal stages in the development of the chick embryo. *Journal of Morphology* 88: 49–92.
- He, B., Doubrovinski, K., Polyakov, O. & Wieschaus, E. 201). Apical constriction drives tissue-scale hydrodynamic flow to mediate cell elongation. *Nature* 508(7496): 392–396.

- Hu, N. & Clark, E. B. 1989. Hemodynamics of the stage 12 to stage 29 chick embryo. *Circ Res* 65(6): 1665–70.
- Jones, E. A., le Noble, F. & Eichmann, A. 2006. What determines blood vessel structure? genetic prespecification vs. hemodynamics. *Physiology (Bethesda)* 21: 388–395.
- le Noble, F., Fleury, V., Pries, A., Corvol, P., Eichmann, A. & Reneman, R. 2005. Control of arterial branching morphogenesis in embryogenesis: go with the flow. *Cardiovascular Research* 65(3): 619–628.
- le Noble, F. I., Moyon, D., Pardanaud, L., Yuan, L., Djonov, V., Matthijsen, R., Bréant, C., Fleury, V. & Eichmann, A. 2004. Flow regulates arterial-venous differentiation in the chick embryo yolk sac. *Development (Cambridge, England)* 131(2): 361–375.
- Lucitti, J. L., Jones, E. A. V., Huang, C., Chen, J., Fraser, S. E. & Dickinson, M. E. 2007. Vascular remodeling of the mouse yolk sac requires hemodynamic force. *Development (Cambridge, England)* 134(18): 3317–3326.
- Manoussaki, D., Lubkin, S. R., Vernon, R. B. & Murray, J. D. 1996. A mechanical model for the formation of vascular networks in vitro. *Acta Biotheor* 44(3-4): 271–82.
- Mobbs, I. & McMillan, D. 1979. Structure of the endodermal epithelium of the chick yolk sac during early stages of development. *Am. J. Anat* 155(3): 287–309.
- Nagai, H. & Sheng, G. J. 2008. Definitive erythropoiesis in chicken yolk sac. *Developmental Dynamics* 237(11): 3332–3341.
- Nguyen, T.-H., Eichmann, A., le Noble, F. & Fleury, V. 2006. ‘Dynamics of vascular branching morphogenesis: The effect of blood and tissue flow. *Phys. Rev. E* 73: 061907.
- Park, C., Kim, T. M. & Malik, A. B. 2013. Transcriptional regulation of endothelial cell and vascular development. *Circ. Res.* 112(10): 1380–1400.
- Popović, M., Nandi, A., Merkel, M., Eournay, R., Eaton, S., Jülicher, F. & Salbreux, G. (2016), Active dynamics of tissue shear flow. *ArXiv* .
- Potente, M., Gerhardt, H. & Carmeliet, P. 2011. Basic and therapeutic aspects of angiogenesis. *Cell* 146(6): 873–887.
- Rachev, A., Stergiopoulos, N. & Meister, J. J. 1996. Theoretical study of dynamics of arterial wall remodeling in response to changes in blood pressure. *Journal of Biomechanics* 29(5): 635–642.
- Rasband, W. S. (1997-2016), ‘ImageJ’, U. S. National Institutes of Health, Bethesda, Maryland, USA, <https://imagej.nih.gov/ij/>.
- Ribatti, D. (2006), Genetic and epigenetic mechanisms in the early development of the vascular system. *J. Anat.* 208(2): 139–152.
- Ribatti, D. & Crivellato, E. 2012. “sprouting angiogenesis”, a reappraisal, *Dev. Biol.* 372(2): 157–165.
- Romanoff, A. 1960. The avian embryo, structural and functional development. MacMillan and Co.
- Sabin, F. R. 1920. Studies on the origin of blood-vessels and of red blood-corpuses as seen in the living blastoderm of chicks during the second day of incubation. *Contributions to Embryology* 9(27/46): 215–U56.

- Sheng, G. 2010: Primitive and definitive erythropoiesis in the yolk sac: a bird's eye view. *Int. J. Dev. Biol.* 54(6-7): 1033–1043.
- Swift, M. R. & Weinstein, B. M. 2009. Arterial-venous specification during development. *Circ. Res.* 104(5): 576–588.
- Taber, L. A. 1998. A model for aortic growth based on fluid shear and fiber stresses. *Journal of biomechanical engineering* 120(3): 348–354.
- Thoma, R. 1893. Untersuchungen über die Histogenese und Histomechanik des Gefäßsystems., Ferdinand Enke.

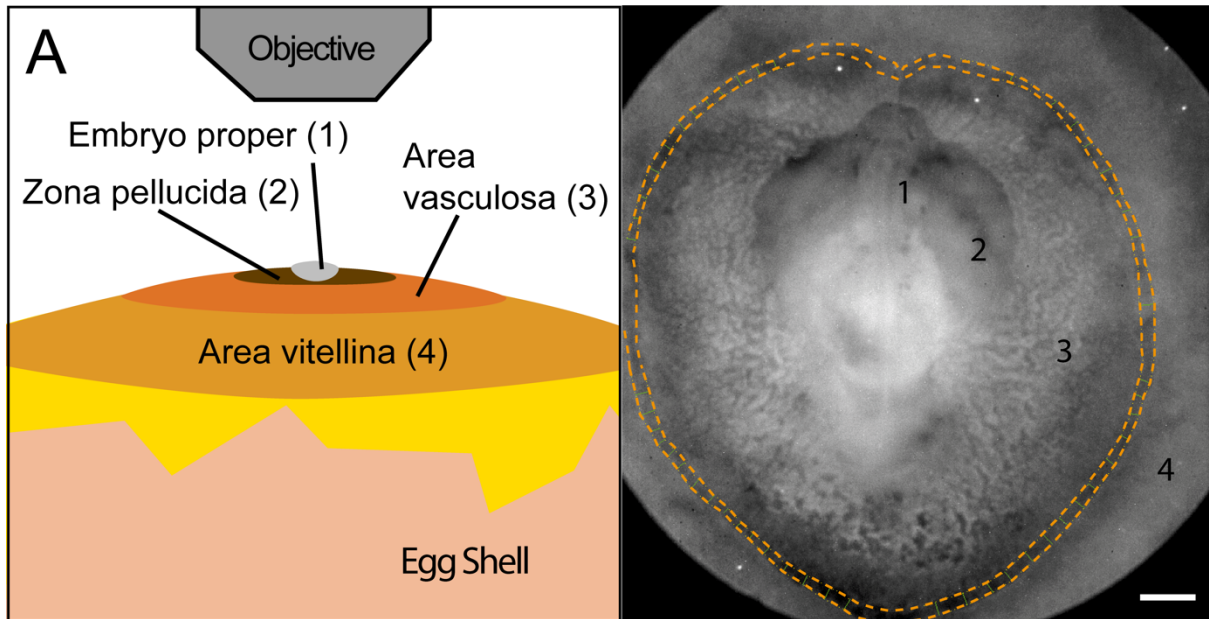


**Figure 1:** A. Schematics of the set up and side view of the chicken embryo and the yolk sac tissues. The embryo proper (1) is surrounded by the zona pellucida (2), which in turn is surrounded by the area vasculosa of the yolk sac (3) in which the mesoderm is present and the blood vessels develop. The area vasculosa is surrounded by the area vitellina (4), in which no mesoderm is present yet. The yolk sac tissues 2-4 form a flat, round layer on the egg yolk. B. Top view of the embryo and yolk sac before the sinus vein is formed, and prior to heart perfusion (HH13). The sinus vein is in between the two orange dotted lines. Scale bar is 1 mm.

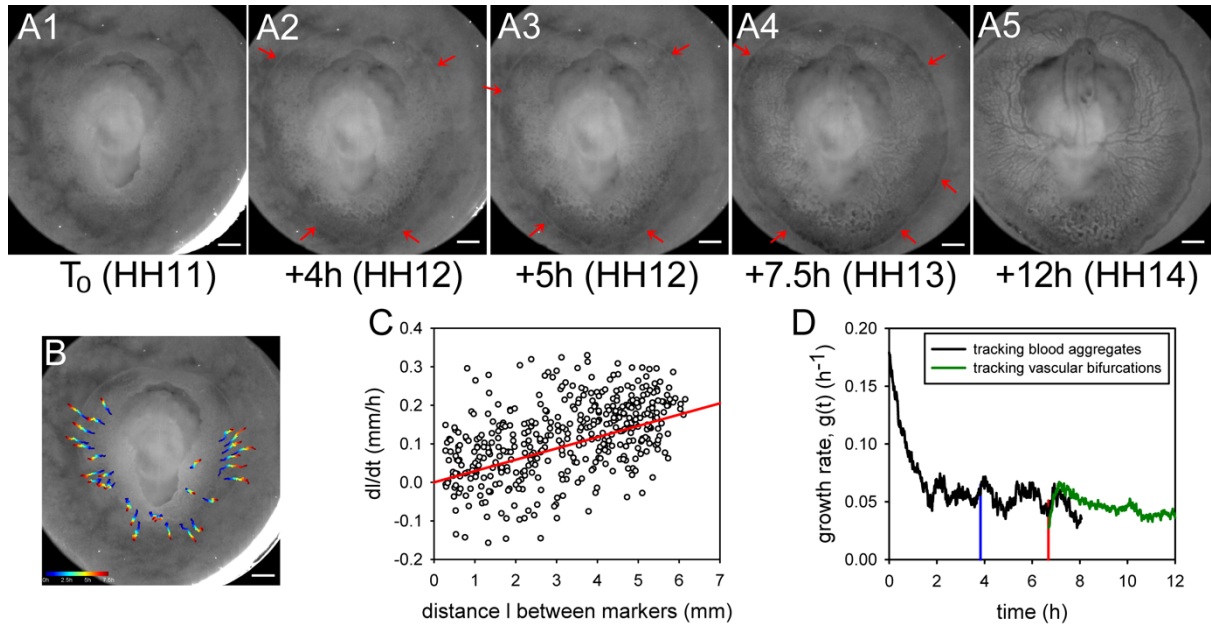


**Figure 2:** A. Formation of the sinus vein. Blood progressively accumulates at the periphery of area vasculosa of the yolk sac (A2-A3, red arrows). When the heart contracts sufficiently efficient, circulation starts and the sinus vein and the other vessels remodel to form a hierarchical vascular network (A4-A5). Extraction of 5 frames of a time lapse movie of 20h with frame rate 60 images/h (Supplemental materials: M1). Scale bar is 1mm. B. Trajectories of the tracked points between 0 and 7.5 hours, superimposed on a frame of the timelapse video at  $T_0$ . Growth causes radial displacements. C.  $\Delta l/\Delta t$  as a function of  $l(t)$  at  $t=2h22'$ .  $l(t)$  is the distance between each pair of tracked points. The associated growth rate equals  $0.029h^{-1}$  and the coefficient of determination  $r^2$  equals 0.24. D. Growth rate  $g(t)$  extracted from linear fits of  $\Delta l/\Delta t$  vs  $l(t)$  performed over the entire experiment. The vertical blue line indicates the time of the first noticeable heart contractions and the onset of visible blood accumulation, which occur approximately at the same time ( $t = 3h50'$ ). The vertical red line shows the onset of blood circulation ( $t = 6h50'$ ) (see also Movie 1).

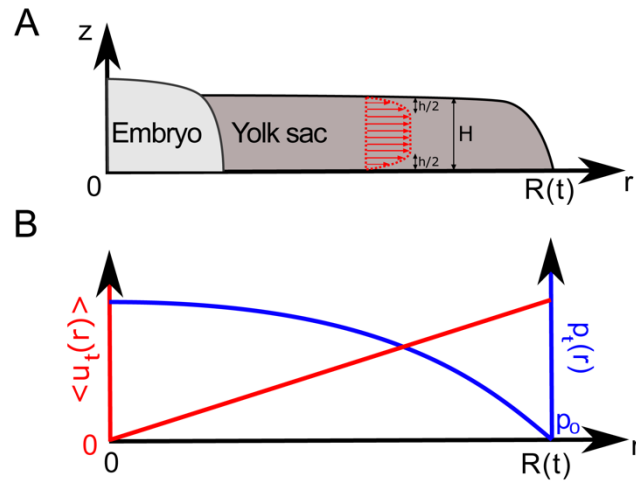


**Figure 3:** A. Schematics of the growth-induced flow. As the yolk sac tissue grows, the tissue flows radially. The mesoderm is a thin layer flowing between the ectoderm and the endoderm, the  $z$ -profile is unknown and could vary from a parabolic profile to a plug profile. The velocity profile depends on  $A$ , the ratio between max and mean velocity, and on  $h$ , the total height of the mesoderm on which there is shear.  $H$  is the mesodermal thickness. In the model the velocity at radius  $r$  is averaged over  $z$ . B. Mean tissue velocity  $u_t(r)$  increases linearly with the distance  $r$  to the center of the embryo, while the pressure  $p_t$  is maximum at the center and decreases with the radius  $r$ .

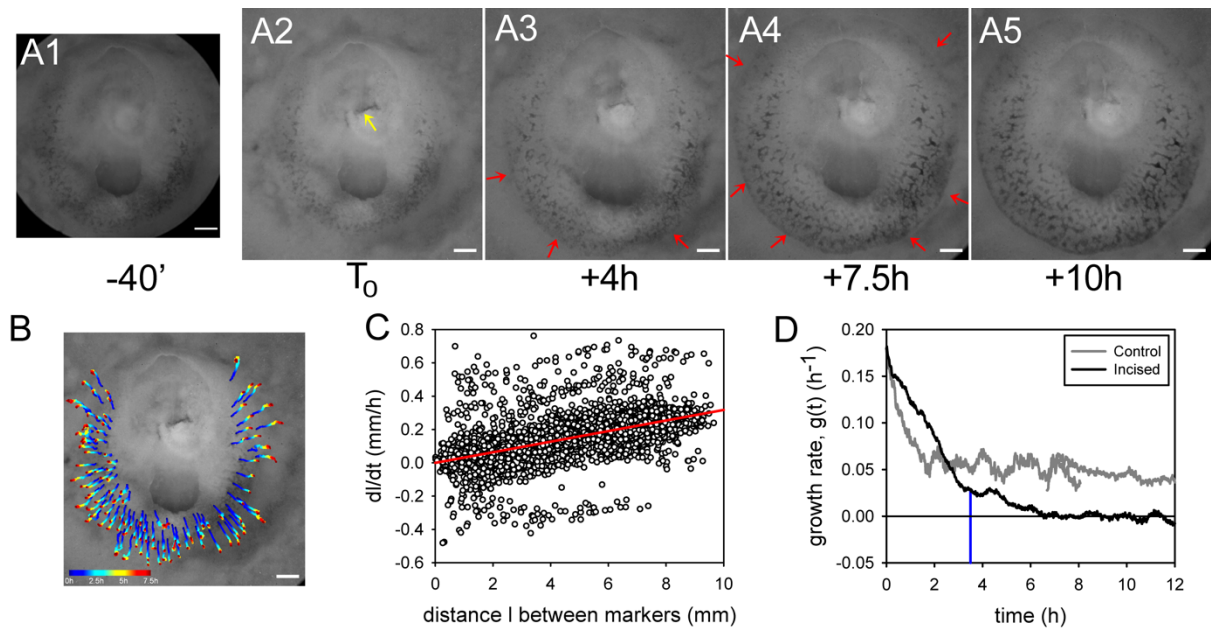


**Figure 4:** A. Yolk sac development for the incised embryo. A1 shows the yolk sac 40 minutes before incision. A2-A5 show the yolk sac development after incision. The yellow arrow in A2 indicates the incision. While the yolk sac still grows, growth is slower than in the control, and eventually stops (A4-A5). Blood accumulation can yet be observed, after about 3.5 hours (A3-A4, red arrows). Extraction of 5 frames of a time lapse movie of 15.5h with frame rate 60 images/h (Supplemental materials: Movie 2). Scale bar is 1mm. B. Trajectories of the tracked points between 0 and 7.5 hours, superimposed on a frame of the timelapse video at  $T_0$ . Growth causes radial displacements. C.  $\Delta l/\Delta t$  as a function of  $l(t)$  at  $t=2h22'$ .  $l(t)$  is the distance between each pair of tracked points. The associated growth rate equals  $0.063h$  and the coefficient of determination  $r$  equals 0.35. D. Black line: Growth rate  $g(t)$  extracted from linear fits of  $\Delta l/\Delta t$  vs  $l(t)$  performed over the entire experiment. The growth rate becomes negative beyond 11.5 hours, as the embryo and yolk sac start to shrink. The vertical blue line indicates the onset of noticeable blood accumulation in the periphery of the area vasculosa. Grey line: Growth rate of the control embryo. The start of the control experiment is shifted such that the initial growth rates for control and incised embryos are the same.

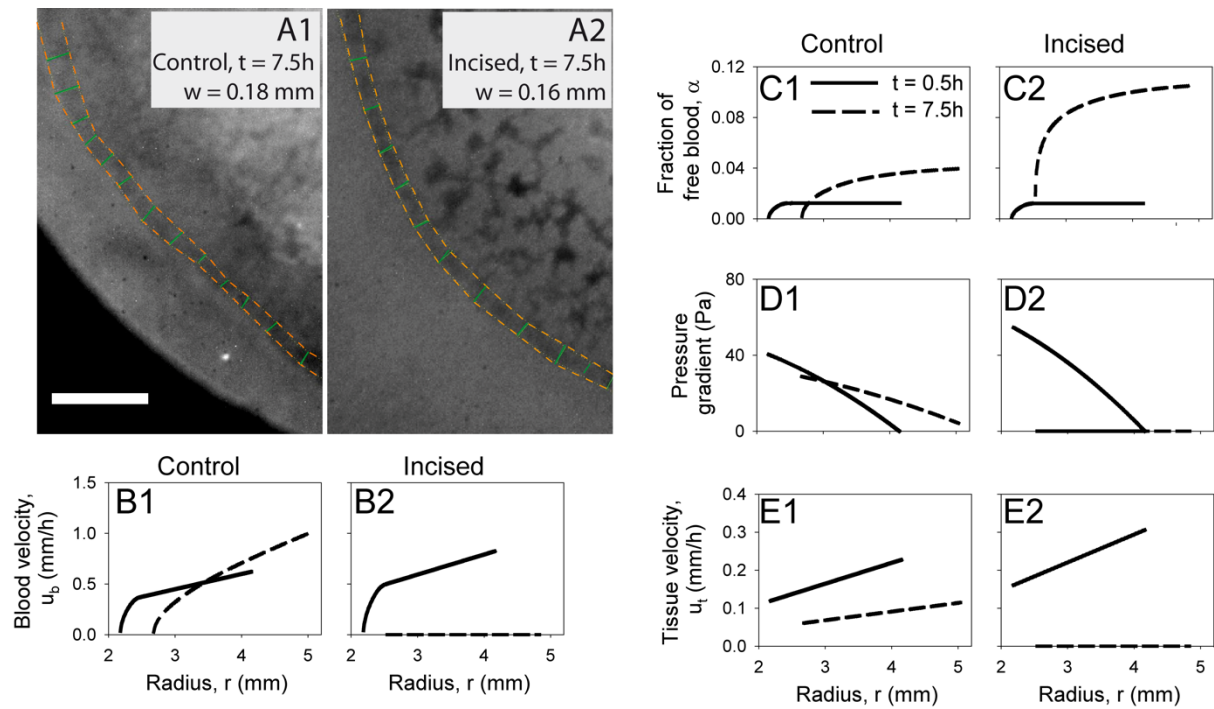


**Figure 5:** A: Measurements of the width of the sinus vein at  $t = 7.5h$  for the control (A1) and incised (A2) embryo. Scale bar is 1 mm. B-E: model variables (blood velocity,  $u_b$  (B), tissue fraction of free flowing blood,  $\alpha$  (C), tissue pressure,  $p_t$  (D) and tissue velocity,  $u_t$  (E)) as a function of position in the yolk sac,  $r$  at  $t = 0.5h$  (solid line) and at  $t = 7.5h$  (dashed line). B1-E1: show the variables using the experimental control growth curve. B2-E2 show the variables using the experimental growth curve for the incised embryo.

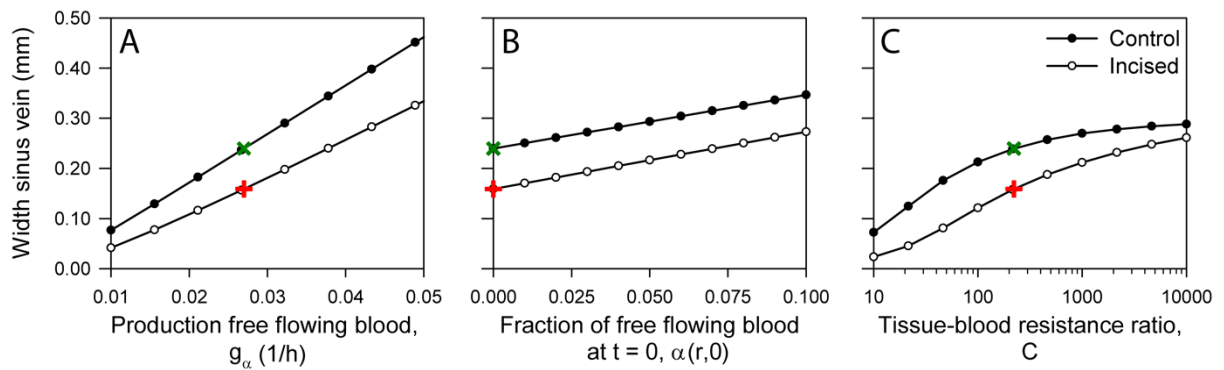


**Figure 6:** Sensitivity analyses for the production of free flowing blood,  $g_\alpha$  (A), for the fraction of free flowing blood at  $t = 0$ ,  $\alpha(r, 0)$  (B) and for the tissue-blood resistance ratio, C (C). Filled circles show simulations with the control growth curve and open circles show simulations with the growth curve for the incised embryo.  $g_\alpha$  is calibrated to the measured width of the sinus vein of the incised embryo (red +). Using the same parameters except for the growth rate, the predicted width, a measure for blood volume accumulation solely due to tissue growth, for the sinus vein in the control is higher (green X).

**Movie 1:** [click here](#)

Time lapse sequence for a control embryo. Orange circles show the tracked trajectories; yellow squares show the predicted position of the moving front of the mesoderm. Scale bar is 1mm. The graph on the right shows the corresponding growth rate curve. The vertical blue line indicates the time of the first noticeable heart contractions and the onset of visible blood accumulation in the periphery of the area vasculosa, which occur approximately at the same time. The vertical red line shows the onset of circulation. When the heart contracts sufficiently efficient, circulation starts and the sinus vein and the other vessels remodel to form a hierarchical vascular network. Sliding vertical black line is time. The full resolution time lapse movie is available upon request.

**Movie 2:** [click here](#)

Time lapse sequence for an incised embryo. Orange circles show the tracked trajectories; yellow squares show the predicted position of the moving front of the mesoderm. Scale bar is 1mm. The graph on the right shows the corresponding growth rate curve. Vertical blue line shows the onset of visible blood accumulation in the periphery of the area vasculosa. Sliding vertical black line is time. The full resolution time lapse movie is available upon request.

## Tables

	Symbol	Relation	Value
<b>VARIABLES</b>			
radial coordinate	$r$		
time	$t$		
tissue velocity	$u_t(r,t)$		
tissue pressure	$p_t(r,t)$		
blood velocity	$u_b(r,t)$		
free blood volume fraction in the mesentery	$\alpha(r,t)$		
transport space fraction in the mesentery	$\psi(r,t)$	$= \alpha(r,t)$	
<b>PARAMETERS</b>			
tissue growth rate	$g(t)$		Fig. 2D / 4D
yolk sac radius at zona pelucida at $t = 0$	$R_{ZP}(0)$		2.1 mm
yolk sac radius at sinus vein at $t = 0$	$R_{AV}(0)$		4.0 mm
resistance to tissue flow	$\Omega_t$	$= \frac{8\eta_t}{Ah^2}$	$4.3 \cdot 10^5 \frac{Pa \cdot s}{m^2}$
tissue velocity profile ratio	$A$	$= \frac{3H-h}{3H}$	$\left[ \frac{2}{3}, 1 \right]$
yolk sac mesodermal thickness	$H$		35 $\mu m$
height of the mesoderm on which there is a shear	$h$		$\langle 0, H \rangle$
tissue viscosity in the shear layers	$\eta_t$		$\langle 0, 43 Pa \cdot s \rangle$
permeability	$\kappa$	$= \frac{\psi b^2}{96}$	
effective pore size	$b$		10 $\mu m$
blood viscosity	$\eta_b$		$2 \cdot 10 Pa \cdot s$
tissue-blood resistance ratio	$C$	$= \frac{\Omega_t b^2}{96\eta_b}$	222
free blood volume fraction at $t = 0$	$\alpha(r, 0)$		0
free blood creation rate	$g_\alpha$		$0.027 h^{-1}$

**Table 1:** Variables and parameters used in the model. The values or ranges of values of the parameters are discussed in the discussion section and in the supplemental materials

# Supplemental material to

## Tissue growth pressure drives early blood flow in the chicken yolk sac

Raphaël Clément, Benjamin Mauroy,  
Annemiek J.M. Cornelissen

### Formulation of a flattened parabolic flow profile

We approximate the flow as two half parabola at the bounding membranes (where there is shear) and flat in the middle (where there is no shear, see Fig. 3 in the manuscript). The parameter  $h$  is the total height on which there is a shear. For a parabolic Poiseuille flow profile,  $h$  equals the total height of the mesodermal tissue ( $H$ ). For a perfect plug flow  $h$  approaches 0.

The radial flux is the sum of the flux for the parabolic part:  $\frac{h^3}{12\eta_t} \text{grad } p_t(r, t)$  and the flux in the plug:  $(H - h)u_{t,max} = (H - h) \frac{h^2}{8\eta_t} \text{grad } p_t(r, t)$ . With  $\eta_t$  being the viscosity in the sheared layers. The average velocity becomes then:

$$u_t = \frac{h^2}{8\eta_t} \frac{3H - h}{3H} \text{grad } p_t(r, t)$$

and the maximum velocity becomes:

$$u_{t,max} = \frac{h^2}{8\eta_t} \text{grad } p_t(r, t).$$

We call  $A$  the ratio between the average and maximum velocity:

$$A = \frac{u_t}{u_{t,max}} = \frac{3H-h}{3H}.$$

### Tissue velocity profile ratio, $A$ and the height of the mesoderm that encounters shear, $h$

$A$  is the ratio between the mean velocity,  $u_t$ , and the maximum velocity.  $A = 2/3$  for a parabolic flow profile (Poiseuille flow) and  $A = 1$  for a perfect plug flow.  $h$  is the total height on which there is a shear. With  $H$  being the thickness of the yolk sac mesoderm, then  $h = H$  for a parabolic flow and  $h = 0$  for a perfect plug flow ( $A = \frac{3H-h}{3H}$ ). The actual shape of the tissue velocity profile is unknown and depends on the friction the yolk sac tissues encounter. There are two sources of friction: the friction inside the tissue between the mesodermal cells

and the friction between the mesoderm and the ecto- and endodermal layers. When they are approximately the same, or when the friction between the mesodermal cells is lower, it approaches a parabolic velocity profile. When there is more friction between the mesodermal cells than at the interfaces the velocity profile flattens up and can, at the other extreme, reach a perfect plug flow. The pressure gradient derived from a parabolic flow is then the lower possible limit, and when the tissue becomes more rigid the pressure gradient can become much larger.

### **Mesodermal thickness, $H$**

Mobbs and Mc Millan 1978, did an anatomical study on the chicken yolk sac. They observed one  $\mu\text{m}$  thick cross sections of epon-embedded HH1 to HH15 yolk sac with toluidine blue staining. The average thickness is about  $35\mu\text{m}$ .

### **Tissue viscosity in the shear layers, $\eta_t$**

When the velocity profile is parabolic ( $A = 2/3$  and  $h = H$ ) the tissue viscosity,  $\eta_t$  describe the global viscosity in the mesoderm. Forgacs et al 1998 used a parallel plate compression apparatus to deform cell aggregates from limb, heart, liver and neural retina of chicken embryos at respectively, 3.5, 5, 5 and 6 embryonic days. For heart, liver and neural retina they estimate a viscosity of  $10^4 \text{ Pa}\cdot\text{s}$ . For the limb they measure  $10^5 \text{ Pa}\cdot\text{s}$ . We expect that the early mesentery mesenchymal tissue has a lower viscosity than these tissues.

When the velocity profile flattens, which is most likely the case, the tissue viscosity,  $\eta_t$  reflects the viscosity in the shear layers.

The value depends on the assumed resistance to tissue flow,  $\Omega_t$  and the tissue velocity profile with parameters  $A$  and  $h$ . The possible values are discussed in the discussion section.

### **Resistance to tissue flow, $\Omega_t$**

The resistance to tissue flow is set to  $4.3 \cdot 10^5 \text{ Pa}\cdot\text{s}/\text{mm}^2$ . The resistance to tissue flow is tuned such that the temporal average of tissue pressure near the embryo ( $r = R_{ZP}$ ) equals the diastolic pressure in the vitelline artery (0.03 kPa) measured at the moment the primary heart starts to contract at HH12 (Hu & Clark 1989).

### **Viscosity of blood, $\eta_b$**

The value of the viscosity of the blood that is flowing was set at  $2\text{mPa}\cdot\text{s}$ . Viscosity of blood depends on the hematocrit level and on the shear rate to which the blood is exposed. In tubes, when blood is moving slowly at low share rates blood cells interact with one and another by forming linear aggregates, the so called rouleaux. The formation of rouleaux increases the apparent viscosity. In the chicken embryo Al-Roubaie et al. measure a hematocrit of 19.4 % at stage HH22. At stage HH11 the hematocrit level is likely lower. They show that at high, unphysiological hematocrit levels ( $> 36\%$ ) the viscosity rises exponentially when share rate is below  $200 \text{ s}^{-1}$ . This shear thinning effect fades at lower hematocrit levels ( $< 17\%$ ), however due to technical limitations they could not measure the viscosity at shear rates lower than  $200 \text{ s}^{-1}$ . Our simulations reveal that shear rates ( $= 8 \times u_b/b$ ) are very low, varying between 0 and  $1 \text{ s}^{-1}$ . Therefore, to account for a possible shear thinning effect we chose a viscosity somewhat

higher than the value ( $1.24\text{mPa}\cdot\text{s}$ ) measured by Al-Roubaie et al at a shear rate of  $200\text{ s}^{-1}$  and at 5 % hematocrit.

### **Effective pore size, $b$**

We set the effective pore size to the diameter of the smallest length scale of the capillary plexus, which we assume is the capillary diameter. Chicken primary red blood cells are oval and 8 by 12.7 microns (Sheng 2010). Besides they have a nucleus and they cannot deform like mammalian red blood cells without nucleus ( $6 - 8\ \mu\text{m}$ ) that can travel through capillaries as small as  $5\ \mu\text{m}$ . Measurements in our lab of capillary diameter at HH17 are in the order of  $10\ \mu\text{m}$ .

### **References**

- Al-Roubaie, S., Jahnsen, E.D., Mohammed, M., Henderson-Toth, C., and Jones, E. A. V. 2011. Rheology of embryonic avian blood. *Am J Physiol Heart Circ Physiol* 301: H2473–H2481
- Forgacs, G., Foty, R.A., Shafrir, Y. & Steinberg, M.S. 1998. Viscoelastic properties of living embryonic tissues: a quantitative study. *Biophysical journal* 74(5): 2227-2234.
- Hu, N. & Clark, E. B. 1989. Hemodynamics of the stage 12 to stage 29 chick embryo. *Circ Res* 65(6): 1665–70.
- Mobbs, I. & McMillan, D. 1979. Structure of the endodermal epithelium of the chick yolk sac during early stages of development. *Am. J. Anat* 155(3): 287-309.
- Sheng, G. 2010. Primitive and definitive erythropoiesis in the yolk sac: a bird's eye view. *Int. J. Dev. Biol.* 54(6-7): 1033-1043.